Impacts of urban stressors on freshwater biofilms

Romain VRBA[1,2 *], Isabelle LAVOIE[2], Nicolas CREUSOT[1], Mélissa EON[1], Débora MILLAN-NAVARRO[1], Agnès FEURTET-MAZEL[3], Nicolas MAZZELLA[1], Aurélie MOREIRA[1], Dolors PLANAS[4], Soizic MORIN[1]

[1] INRAE, UR EABX, 50 avenue de Verdun, 33612 Cestas cedex, France

[2] INRS-ETE, 490 rue de la Couronne, Québec, QC G1K 9A9, Canada

[3] Univ. Bordeaux, UMR CNRS 5805 EPOC-OASU, F-336120 Arcachon, France

[4] UQAM, GRIL-Département des sciences biologiques, 141 Avenue du Président-Kennedy, Montréal, QC H2X 1Y4, Canada

*Corresponding author at: INRAE, UR EABX, 50 avenue de Verdun, 33612 Cestas cedex, France.

Tel. : +33 6 95 43 84 28

E-mail address: romvrba@outlook.fr

Graphical abstract

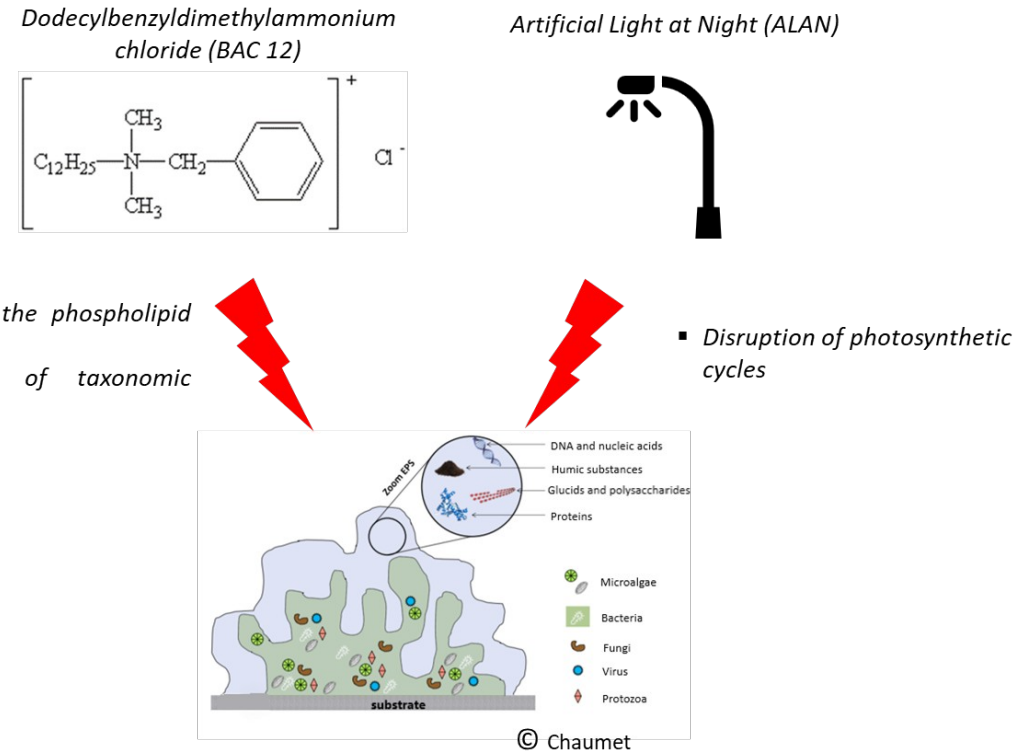

Abstract

In urban areas, aquatic ecosystems and their communities are exposed to numerous stressors of various natures (chemical and physical), which impacts are often poorly documented. In epidemic context such as the COVID 19 pandemic, the use of biocides such as the dodecylbenzyldimethylammonium chloride (BAC 12) increased, resulting in an expectable increase in their concentrations in urban aquatic ecosystems. This compound is known to be toxic to most aquatic organisms. Besides, artificial light at night (ALAN) is increasing globally, especially in urban areas. ALAN may have a negative impact on photosynthetic cycles of periphytic biofilms, which in turn may result in changes in their metabolic functioning. Moreover, studies suggest that exposure to artificial light could increase the biocidal effect of BAC 12 on biofilms. The present study investigates the individual and combined effects of BAC 12 and/or ALAN on the functioning and structure of photosynthetic biofilms. We exposed biofilms to a nominal concentration of 30 mg.L-1 of BAC 12 and/or ALAN for 10 days. BAC 12 had a negative impact on biofilm functioning by decreasing the amount and the quality of photosynthetic pigments, resulting in a >90% decrease in photosynthetic efficiency after 2 days of exposure. We also noted a strong decrease in glycolipids that resulted in a shift in lipid profiles. We found no significant effect of ALAN on the endpoints assessed and no interaction between the two stress factors.

Keywords: Biocide, ALAN, biofilm, photosynthetic efficiency, bioaccumulation, lipids.

1- Introduction

Today, biocides are widely used in different areas of activity including agriculture and industry, as well as in a multitude of products (e.g. pharmaceutical, personal care and household products) (Abbott et al., 2020). Among these biocides, dodecylbenzyldimethylammonium chloride (BAC 12), a quaternary ammonium compound, is commonly used as an active substance in medical disinfection products, as well as in household products such as detergents. Recently, following the regulation of some broadly used disinfectant agents such as triclosan, quaternary ammonium compounds like BAC 12 have become popular substitutes (Sreevidya et al., 2018). Moreover, BAC 12 and all other benzalkonium chloride derivatives have been shown to be very effective against the SARS-CoV virus (Rabenau et al., 2005), resulting in their widespread use as disinfectants during pandemic. For example, benzalkonium chloride-based disinfectants represented more than half of the products recommended by the US Environmental Protection Agency (EPA) against SARS-CoV-2 (US EPA, 2020).

Like other contaminants, BAC 12 eventually reaches wastewaters, where its concentration varies greatly depending on the land use, population and wastewater treatment facilities, among other factors. For example, a concentration of 6 $mg.L^{-1}$ was recorded in hospital effluents (Kümmerer et al., 1997) due to the intensive use of BAC 12 as a disinfectant. In municipal wastewater effluents, BAC 12 concentrations were observed to range from just a few $ng.L^{-1}$ up to 170 $\mu g.L^{-1}$ (Clara et al., 2007; Martínez-Carballo et al., 2007; Zhang et al., 2015). BAC 12 concentration was likely much higher during the Covid-19 pandemic as a result of increased efforts to sanitize all kinds of surfaces. According to the US EPA, BAC 12 is

relatively stable to photodegradation and its half-life in surface waters can reach 180 days, although the presence of photosensitizers can reduce this half-life to a week (US EPA, 2006). The K_{oc} of BAC 12 is 5.43 and, therefore, it has a high adsorption ratio on sewage sludge, sediments or humic substances (van Wijk et al., 2009). However, some bacterial strains in wastewaters, such as *Aeromonas hydrophila*, can biodegrade the BAC 12 molecule and use the ammonium as a source of nitrogen (Patrauchan and Oriel, 2003).

The toxicity of BAC 12 to cells is due to its quaternary ammonium polar head, which has the capacity to bind to the surface membrane, while the alkyl lipophilic chain alters the phospholipid bilayer. This alteration can rapidly lead to membrane disruption and progressive lysis of the cell (Eich et al., 2000). BAC 12 has attracted attention in medical research because of its widespread use, as some bacterial strains such as *Staphylococcus aureus* (Wassenaar et al., 2015) have shown resistance mechanisms. Resistant strains of *Pseudomonas aeruginosa* show some differences in their fatty acid profiles that induce shifts in cell membrane composition (Sakagami et al., 1989; Kim et al., 2018).

Although the transfer of BAC 12 to aquatic ecosystems has been recognized, the ecotoxicity of BAC 12 to aquatic organisms is poorly documented. There is redundancy in the organisms used for toxicity assessment, since most studies have focused on *Daphnia magna* to determine the toxicity of BAC 12 (Kreuzinger et al., 2007; Leal et al., 1994; Chen et al., 2014; Lavorgna et al., 2016). To date, *D. magna* is the most sensitive organism to BAC 12, where the concentration needed to immobilize 50% of organisms (EC_{50}) has been shown to be 5.9 $\mu g.L^{-1}$ (US EPA, 2006). As a result, the US EPA established a non-observed adverse effect concentration (NOAEC) of 4.15 $\mu g.L^{-1}$ for aquatic invertebrates. Phytoplanktonic organisms seem to be less sensitive to BAC 12 than aquatic invertebrates. Indeed, several other studies investigated the effects of BAC 12 on various microalgae species and the range of EC_{50} based on growth was found to vary between 58 $\mu g.L^{-1}$ for *Skeletonema costatum* (Kreuzinger et al., 2007) to 203 $\mu g.L^{-1}$ for *Chlorella vulgaris* (Sütterlin et al., 2008).

In this study, we focused on stream biofilms (periphyton), which are complex structures housing autotrophic microorganisms (e.g. cyanobacteria, green algae, diatoms), bacteria, fungi, and other heterotrophic organisms. Biofilms are ubiquitous in aquatic environments, including urban streams and ponds. They can also be found downstream of wastewater treatment plants (WWTPs) and have been used to detect structural and functional changes as a response of microbial communities to stress (Tamminen et al., 2022; Tlili et al., 2020). Diatoms are often the major algal components in biofilms in terms of biomass (Morin et al., 2016). Diatoms are rich in essential polyunsaturated fatty acids such as eicosapentaenoic acid (EPA) (Zulu et al., 2018), ensuring a high nutritional quality of this primary resource for biofilm consumers. Changes in the biofilm community structure could lead to a decrease in essential polyunsaturated fatty acids (Brett and Müller-Navarra, 1993). Recent studies also demonstrated that diatom fatty acid composition can be altered by organic substances such as pesticides (Demailly et al., 2019). Given the toxic mode of action of BAC 12, impacts on biofilm fatty acids, particularly membrane phospholipids, are likely to occur. The attack on phospholipid membrane may also result in the disruption of key functions of biofilm such as photosynthesis for example, Pozo-Antonio and Sanmartin (2018) showed a significant decrease in chlorophyll *a* and photosynthetic efficiency of phototrophic biofilms from church

walls after a BAC 12 treatment. The effect of BAC 12 as a biofouling removal agent was significantly enhanced when combined with artificial light or UV irradiation.

With urban development, artificial light at night (ALAN) has become a global pollution concern and more than 80% of the world population lives under a light-polluted sky (Falchi et al., 2016). Furthermore, most urban areas have developed along rivers and coastlines, increasing the exposure of aquatic environments to ALAN. Concerns about the impact of ALAN on aquatic ecosystems and research on this topic are quite recent (Perkin et al., 2011). Indeed, ALAN was only recognized as harmful for freshwater ecosystems in the early 2000s (Longcore and Rich, 2004). ALAN could lead to disruptions in photosynthesis-respiration cycles of autotrophic organisms in biofilms by inducing variability in the maximum efficiency of photosynthesis (Maggi and Serôdio, 2020). ALAN can also alter taxonomic composition by favouring certain autotrophic groups over others, thereby exerting differential selection, as shown in a study where cyanobacteria proportions in biofilm decreased under ALAN (Grubisic et al., 2017).

The objectives of this study were to determine (1) the individual and combined effects of urban stressors (BAC 12 and continuous light) on autotrophic organisms within the biofilm (i.e. photosynthetic efficiency and lipid composition), and (2) the impact of these two stressors on the taxonomic composition of the biofilm and the consequences for the proportion of essential fatty acids, which could result in a decrease in the nutritional value of this basal resource.

2- Material and methods

2.1- Experimental design

Biofilms were grown in a small pond in Cestas, near Bordeaux, France. Glass slides were immersed at a depth of 30-50 cm for a colonization period of five months (December 2020 to April 2021). A previous study classified this small water body as a hypereutrophic pond (Chaumet et al., 2019; Neury-Ormanni et al., 2020). At the end of the colonization period, the glass slides covered by mature biofilms were randomly distributed among four series of

Experimental Units (EU) for the trial. The EUs consisted of aquaria of about 30 L filled with pond water previously filtered (20 µm) to remove suspended material and most planktonic organisms. The slides were divided among three parallel channels per EU, connected to 10-L tanks. In each channel, 12 colonized glass slides were placed for subsequent exposure of the biofilms to the different treatments (BAC 12 and ALAN). Biofilms corresponding to the day 0 (d0) sample were collected immediately after their recovery from the pond.

On d0, two EUs were contaminated with a solution of dodecylbenzyldimethylammonium chloride (BAC 12; Sigma Aldrich, France; CAS: 139-07-1, purity: >99%) to reach a concentration of 30 $mg.L^{-1}$. This concentration had been found to be the EC_5 for biofilm photosynthesis inhibition in a preliminary toxicity experiment to assess BAC 12 toxicity towards pond biofilm (see Appendix A). Light (20 $\mu mol.s^{-1}.m^{-2}$) was kept on overnight and then from day 1 (d1), one control series and one BAC 12 series were exposed to an alternating 14 h day / 10 h night photoperiod (alternated photoperiod, AP) and the other two series (one control, one BAC 12) were exposed to a 24 h day photoperiod (continuous photoperiod, CP) throughout the course of the experiment. Room temperature was maintained constant at 20.5 ± 0.1°C, while water temperature was kept at 18.7 ± 0.2°C. The tanks were refilled with 3 L of filtered pond water contaminated at 30 $mg.L^{-1}$ BAC12 on day 4 (d4) to compensate for water evaporation.

2.2- Water chemistry measurements

On d0, d1, d2, d4, d7 and d10, 20 mL water samples were taken from all channels, filtered on 1-µm PTFE filters and stored at 4°C in the dark until analysis (performed within 48 h of collection). Nutrients and mineral salts were analysed using a Metrohm 881 Compact Ionic Chromatograph pro (Metrohm). Anion analysis (PO_4^-, NO_3^-, NO_2^-, Cl^- and SO_4^{2-}) was performed using a Supp 4/5 Guard/4.0 precolumn followed by a Metrosep A Supp5 – 250/4.0 column. The mobile phase was a mixture of a solution of 3.2 $mmol.L^{-1}$ Na_2CO_3 and a solution of 1 $mmol.L^{-1}$ $NaHCO_3$. Cation analysis (Na^+, K^+, Ca^{2+}, Mg^{2+} and NH^{4+}) was performed using a C4 Guard/4.0 precolumn followed by a Metrosep C6 - 250/4.0 column). All precolumns and columns come from the provider Metrohm. The eluent used was a mixture of 2.5 $mmol.L^{-1}$ HNO_3 and a solution of 1.7 $mmol.L^{-1}$ 10,12-Pentacosadynoic acid (PCDA). The limits of quantification of the different ions analysed are shown in Table 1.

BAC 12 concentrations in the water were monitored frequently over the experiment, at d0, d1, d2, d4, d7 and d10. Three samples of 20 mL were collected from each channel and stored at -20°C together with the stock solution until analysis. The samples were analysed using an Ultimate 3000 HPLC coupled with an API 2000 triple quadrupole mass spectrometer. We used a Gemini® NX-C18 column from Phenomenex as a stationary phase. The mobile phase was 90:10 5 mM ammonium acetate/acetonitrile. We worked in isocratic mode, so the composition of the mobile phase was constant during the analysis. The flow rate was set at 0.6 $mL.min^{-1}$ and the injection volume was set at 20 µL. An internal standard of benzyl-2,3,4,5,6-d5-dimethyl-n-dodecylammonium chloride was used (Cluzeau, France; CAS: 139-07-1, purity: >98%). Samples were diluted and the calibration range was from 1 to 200 $\mu g.L^{-1}$. Quality controls were regularly injected at concentrations of 5 and 25 $\mu g.L^{-1}$, as well as analytical blanks.

186

187 **2.3- Biofilm biological endpoints**

188 ***Photosynthetic efficiency***

189 We sampled 2 cm² of biofilm from three different glass slides for each treatment on d0, d2,
190 d4, d7, and d10, corresponding to three pseudoreplicates per treatment per sampling. Each
191 biofilm sample was then suspended in 3 mL of channel water. Photosynthetic efficiency was
192 assessed within one hour after collection using pulse amplification modulation equipment
193 (Phyto-PAM) from Heinz Walz GmbH. After these photosynthesis measurements, samples
194 were preserved for further microscopic analyses by adding a few drops of Lugol solution
195 then stored in the dark at 4°C.

196 ***Microscopic analyses***

197 For microscopic observations, a Nageotte counting slide (Marienfeld, Germany) was used
198 with 125 µL biofilm suspension samples collected on d0, d2 and d10. Observations were
199 made at x400 magnification under an optical microscope (Olympus BX51) equipped with a
200 digital camera. Ten fields of view were scanned for enumeration of diatoms, green algae,
201 cyanobacteria and micro-meiofauna (e.g. rotifers, ciliates, nematodes). Live (intact cell
202 content) and dead (empty frustules) diatoms were counted separately to estimate mortality
203 (Morin et al. 2010).

204 ***Lipid classes, bioconcentration and pigments***

205 Biofilms were scraped from glass slides on d0, d1, d2 and d10 (4 slides per treatment) and
206 were frozen in liquid nitrogen to prevent lipid degradation. The samples were then
207 lyophilized for 24 hours. Lipids were extracted using a mixture of MTBE-methanol (3:1 %v/v)
208 and UPW-methanol (3:1 %v/v) with 150 mg of microbeads. Biofilm cells (20 mg dry weight)
209 were then homogenized by agitating the samples with FastPrep. The upper organic fraction
210 of the samples (i.e. MTBE) was recovered by centrifugation, while the lower hydrophilic
211 fraction (mixture of UPW and methanol) was used to determine BAC 12 bioaccumulation.
212 For lipid analysis, samples were evaporated and injection solvent was added before analysis
213 by HPLC-MS/MS. Different stationary and mobile phases were used for the analysis of
214 phospholipids/glycolipids and triglycerides. For the phospholipid and glycolipid analyses, a
215 LUNA® NH2 column (100 x 2 mm, 3 µm) from Phenomenex was used as the stationary
216 phase, and a mixture of acetonitrile and 40 mM ammonium acetate buffer as the mobile
217 phase. The flow rate was set at 400 $\mu L.min^{-1}$. The proportions of these two solutions are
218 given in Appendix D. For the analysis of triglycerides and betaine lipids (i.e.
219 diacylglyceryltrimethylhomo-Ser, DGTS), a KINETEX® C8 column (100 x 2.1 mm, 2.6 µm) from
220 Phenomenex was used as the stationary phase, and the mobile phase was a mix of a solution
221 of acetonitrile/water/40 mM ammonium acetate buffer (600/390/10, v/v/v) and a solution
222 of isopropanol/acetonitrile/1 M ammonium acetate buffer (900/90/10, v/v/v). The flow rate
223 was set at 300 $\mu L.min^{-1}$. The proportions of these two solutions are given in Appendix D.
224 Results were then pre-treated with ANALYST® 1.6.2 software from Sciex. For polar lipids (i.e.
225 glycolipids and phospholipids), the limits of quantification ranged from 0.1 to 0.5 $nmol.mg^{-1}$,

depending on the lipid classes. For triglycerides and DGTS, the limits of quantification reached were 0.01 and 0.1 nmol.mg^{-1}, respectively. Results were expressed as nmol.g^{-1} freeze-dried biofilm.

The same analytical method used for water samples was used to determine bioaccumulated BAC 12 in the hydrophilic fraction of the previously extracted biofilm. It was generally necessary to perform significant dilutions (i.e. 10,000-fold) in order to stay within the calibration range. Results were then expressed in the log10 value of the bioaccumulation factor (i.e. log(BCF)). The bioaccumulation factor (BCF) was calculated according to the following formula:

$$BCF = \frac{Concentration of BAC\,12 \in biofilm\,(mg/kg)}{Concentration of BAC\,12 \in water\,(mg/L)}$$

On selected freeze-dried samples, pigment analyses were also performed (see Appendix C). Ten mg of dry biofilm were put in solution using 10 mL of acetone. After 20 minutes of ultrasonication, the mix was filtered on a Büchner filter to remove the solid phase. Absorption was measured at the wavelengths 630 nm, 647 nm, 664 nm, 665 nm and 750 nm and was then remeasured at the same wavelengths after acidification of the samples. The concentrations of chlorophyll pigments and phaeopigments were determined following the equations of Lorenzen (Lorenzen, 1967).

2.4- Data analyses

Data were processed using R software (R Core Team, 2022). One- and two-way ANOVAs were performed (after verification of homogeneity of variances) to assess the effect of light on BAC 12 degradation and nutrient levels in the different treatments. Two-way ANOVAs with repeated measures were applied to assess the effect of BAC 12 and ALAN on biofilm endpoints. We also performed a principal component analysis to present a graphic projection of the different fatty acid profiles.

7

256 # 3- Results

257 ## 3.1- Water chemistry

258 **Table 1. Principal ions and BAC 12 concentrations (mg.L^{-1}) in the four experimental treatments along the ten days exposure. Results are expressed as the mean and**
259 **standard error for the whole experiment. Two-way Anovas were conducted with Light and BAC 12 as the two factors. BAC 12 = contaminated biofilm; CONTROL = non-**
260 **exposed biofilm; AP = alternated photoperiod; CP = continuous photoperiod; LOQ = Limit of quantification.**

261

262

Treatment	BAC 12	NO_2	NO_3	PO_4	SO_4	Cl	NH_4	Na	K	Ca	Mg
CONTROL-AP	<LOQ	0.02 ± 0.01	0.75 ± 0.22	0.03 ± 0.05	17.84 ± 0.68	33.0 ± 1.4	0.10 ± 0.13	18.78 ± 0.89	4.21 ± 0.25	49.5 ± 2.6	4.18 ± 0.20
BAC 12-AP	27 ± 12	0.02 ± 0.01	0.66 ± 0.38	0.03 ± 0.04	18.9 ± 1.8	35.5 ± 3.1	0.11 ± 0.12	19.7 ± 2.0	4.34 ± 0.45	52.2 ± 5.7	4.41 ± 0.45
CONTROL-CP	<LOQ	0.02 ± 0.01	1.35 ± 0.52	0.01 ± 0.01	17.53 ± 0.68	30.27 ± 0.79	0.09 ± 0.14	18.52 ± 0.74	4.12 ± 0.14	48.4 ± 1.5	4.09 ± 0.14
BAC 12-CP	17.2 ± 7.5	0.04 ± 0.06	1.69 ± 0.62	0.03 ± 0.04	21 ± 4	36.4 ± 6.0	0.09 ± 0.12	22.0 ± 4.4	4.80 ± 0.95	57.8 ± 11.5	4.90 ± 0.95
LOQ	0.001	0.005	0.01	0.01	0.005	0.01	0.005	0.01	0.0025	0.15	0.15
Significant factor(s) and interaction(s)	Light	None	BAC 12	NA	BAC 12	BAC 12	NA	BAC 12	NA	BAC 12	BAC 12
p value	2.97e-08	>0.05	3.0e-4	NA	0.026	0.007	NA	0.040	NA	0.035	0.030

8

In the control channels, BAC 12 concentrations were always below detection limit (Table 1), confirming that no cross-contamination occurred. Contaminant concentrations averaged 27 ± 12 $mg.L^{-1}$ (AP) and 17 ± 7 $mg.L^{-1}$ (CP) in the BAC 12 treatments. Differences in BAC 12 concentrations were observed between the BAC 12 treatment channels exposed to an alternated photoperiod and those exposed to a continuous photoperiod ($F_{[1,10]} = 232.72$; $p = 2.97e-08$), suggesting that degradation occurred under the continuous photoperiod. Nutrient concentrations were also modified by BAC 12 exposure (Table 1). Indeed, BAC 12 addition (indirectly via effects on organism) resulted in higher concentrations of NO_3, SO_4, Cl, Na^+, Ca^{2+} and Mg^+ than in the control (Table 4) while light exposed solutions show no effects on nutrient concentrations.

.

9

3.2- Effects of BAC12 and ALAN on biofilm communities

Effects of BAC 12 on photosynthetic efficiency

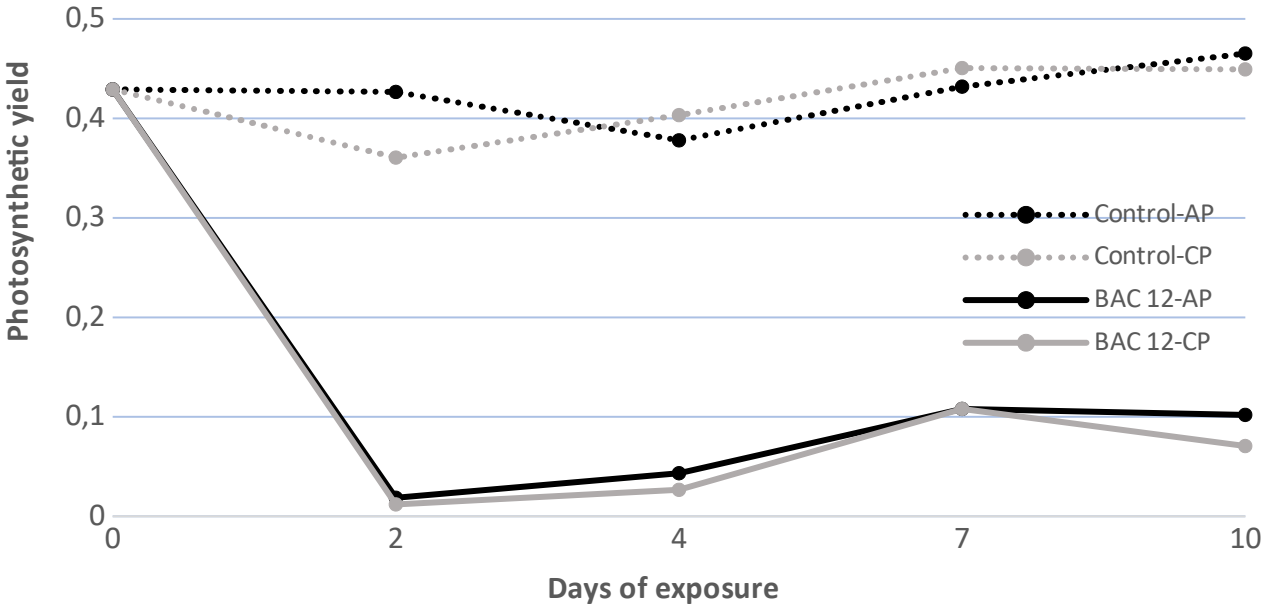

Figure 1. Evolution of photosynthesis yield in biofilms along the ten days of the experiment. BAC 12 = contaminated biofilm; CTRL = non-exposed biofilm; AP = Alternated Photoperiod; CP = Continuous Photoperiod

Figure 1 shows that photosynthetic activity was stable over the experiment, with a mean value of 0.42 ± 0.01 in the control channels, regardless of the light exposure treatment ($F_{[1,42]} = 2.65$; $p > 0.05$). Biofilms exposed to BAC 12 showed an almost complete inhibition of photosynthetic yield starting from d2 and lasting until the end of the experiment ($F_{[1,42]} = 1279$; $p = 4.45e33$). In the same way as for control channels, photosynthetic activity showed no difference between the two light conditions for contaminated channels ($F_{[1,42]} = 0.18$; $p = 0.67$).

10

311 ***Effects on community composition***

Table 2. Evolution of the taxonomic composition of biofilms during the experiment. Densities are expressed as individuals×10^3 / cm^2, i.e. number of cells for microalgae, and number of organisms for microfauna. Diatom mortality is expressed in %. BAC 12 = contaminated biofilm; CTRL = non-exposed biofilm; AP = Alternated Photoperiod; CP = Continuous Photoperiod

312

Date	Treatment	Diatom density	Diatom mortality	Green algae density	Cyanobacteria density	Microfauna density
d0	Control	21.5 ± 5.5	7 ± 6	1.8 ± 1.2	3.2 ±3.2	0.19 ± 0.05
d2	Control-AP	94.2 ± 8.6	3 ± 3	17.8 ± 4.1	1.1 ± 0.2	0.4 ± 0.2
d2	BAC 12-AP	75.5 ± 10.8	3 ± 3	7.9 ± 2.6	0	0.2 ± 0.2
d2	Control-CP	88.0 ± 6.5	3 ± 3	34.5 ± 43.4	0	0.2 ± 0.2
d2	BAC 12-CP	96.7 ± 24.6	2 ± 2	4.2 ± 1.6	0	0
d10	Control-AP	65.5 ± 11.0	5 ± 5	150.4 ± 125.8	7.5 ± 7.4	0.6 ± 0.5
d10	BAC 12-AP	85.7 ± 24.6	2 ± 2	12.6 ± 13.9	3.2 ± 3.2	0
d10	Control-CP	60.9 ± 13.4	6 ± 6	236.1± 78.	0	0.6 ± 0.2
d10	BAC 12-CP	67.3 ± 25.4	1 ± 1	20.5 ± 7.7	0	0
	Significant factor(s) and interaction(s)	None	BAC 12	BAC 12 × Time	None	BAC 12 × Time
	p-value	>0.05	0.031	9.53e-05	>0.05	0.003

Diatoms (91%) dominated the biofilm community at d0 and low proportions of green algae (5%), cyanobacteria (4%) and microfauna (1%) were observed (Table 2). In the control channels, green algae developed markedly and became the main algal group in terms of density by d10, with no significant effect of the photoperiod conditions (e.g. 67% in channels exposed to an alternated photoperiod and 79% in those exposed to a continuous photoperiod). There was also an increase in proportions of green algae in the BAC 12 contaminated channels, although this was not as marked as in the control channels (significant Date × BAC interaction; Table 2). Microfauna numbers increased in control channels, but had completely disappeared from biofilms exposed to BAC 12 by d10 (significant Date × BAC interaction; Table 2). Light conditions did not have a significant impact on the biofilm taxonomic composition.

Diatom mortality (based on the ratio between frustules without cell content and total cell numbers) showed a significant effect of BAC 12 exposure in the AP and CP treatments (Table 2). Note that microscopic observations highlighted differences in the aspect (shape, colour) of chloroplasts in diatoms and chlorophytes exposed to BAC 12, becoming highly granular and darker (Figure B.2). These were, however, not considered as 'dead' cells in estimating diatom mortality.

12

3.3- Impacts of BAC 12 and continuous photoperiod on polar lipids

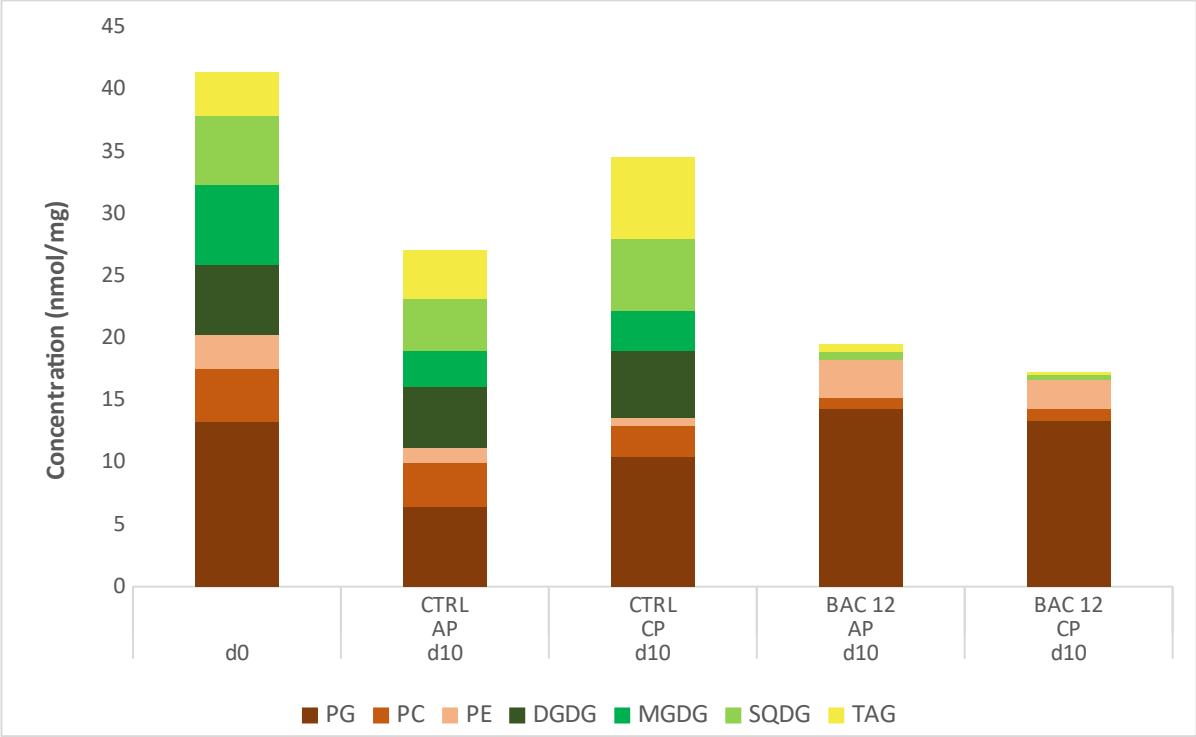

Figure 2. Effects of BAC 12 and continuous photoperiod on the proportion of total lipids and on lipid classes. BAC 12 = contaminated biofilm; CTRL = non-exposed biofilm; AP = alternated photoperiod; CP = continuous photoperiod; PE = phosphatidylethanolamine; PC = phosphatidylcholine; PG = phosphatidylglycerol; DGDG = digalactosyldiacylglycerol; MGDG = monogalactosyldiacylglycerol; SQDG = sulfoquinovosyldiacylglycerol; TAG = triacylglycerides.

On d0, total lipid concentration reached 42.6 nmol.mg^{-1} of freeze-dried biofilm. Almost half of the lipids were phospholipids, and the other half were glycolipids, while neutral lipids (TAG) represented a minor portion (Table 3). By d10, total lipid concentration had decreased in all treatments down to an average of 23.6 ± 7.53 nmol.mg^{-1} of freeze-dried biofilm (Table 3). No significant differences were found between light conditions, while BAC significantly affected glycolipids. As an example, Figure 2 shows lipid profiles under BAC12 exposure and alternated photoperiod on d0 and d10. At the beginning of the experiment, phosphatidylglycerol (PG) was the predominant lipid in the biofilms, although phospholipids and glycolipids in the biofilms were evenly distributed. Although total lipids decreased over time in the controls, the proportions of phospholipids and glycolipids remained similar to those at d0, all the main classes of lipids present. In the samples exposed to BAC 12, glycolipids such as monogalactosyldiacylglycerol (MGDG) and digalactosyldiacylglycerol (DGDG) decreased significantly, or even became barely detectable. Phospholipids, especially PE and phosphatidylglycerol (PG) were higher in biofilms exposed to BAC 12 compared to control (Figure 2, Table 3). Diacylglyceryltrimethylhomo-Ser (DGTS) was never detected and, therefore, is not mentioned further.

13

374

Table 3: Evolution of lipid content of biofilms (in nmol.g-1 freeze-dried biofilm) between the beginning and the end of the experiment. BAC 12 = contaminated biofilm; CTRL = non-exposed biofilm; AP = Alternated Photoperiod; CP = Continuous Photoperiod. Two-ways ANOVA on repeated measure was applied on data.

375

Date	Treatment	Neutral lipids (TAG)	PG	PE	PC	MGDG	DGDG	SQDG	Σ Phospholipids	Σ Glycolipids	Total lipids
d0	**Control**	4.2 ± 2.5	13.7 ± 3.1	2.8 ± 0.5	4.6 ± 0.2	6.4 ± 1.6	5.6 ± 1.2	5.3 ± 1.1	21.0 ± 3.3	17.3 ± 2.4	42.6 ± 3.2
d10	**Control-AP**	3.9 ± 2.0	6.4 ± 1.0	1.3 ± 0.5	3.5 ± 1.5	2.9 ± 0.5	4.8 ± 0.8	4.2 ± 0.7	11.2 ± 2.4	12.0 ± 0.4	27.1 ± 4.1
d10	**BAC 12-AP**	0.2 ± 0.3	14.3 ± 2.6	3.0 ± 0.4	0.9 ± 0.4	0	0	0.7 ± 0.2	18.2 ± 2.6	0.7 ± 0.2	19.1 ± 2.6
d10	**Control-CP**	6.6 ± 2.9	6.9 ± 6.7	0.7 ± 0.1	2.6 ± 1.1	3.3 ± 1.1	5.3 ± 0.2	5.8 ± 1.2	10.1 ± 7.8	14.4 ± 2.2	31.1 ± 8.1
d10	**BAC 12-CP**	0.1 ± 0.1	13.3 ± 3.5	2.3 ± 1.0	1.0 ± 1.0	0	0	0.4 ± 0.2	16.6 ± 5.2	0.4 ± 0.2	17.1 ± 5.3
	Significant factor(s)	BAC 12 × Time	BAC 12× Time	BAC 12× Time	BAC 12× Time	BAC 12× Time	BAC 12× Time	BAC 12× Time	None	BAC 12× Time	BAC 12× Time
	p-value	0.01	0.019	0.002	0.006	0.006	1.22e-06	2.16e-05	>0.05	3.46e-07	8.00e-03

14

3.4- Relationships between taxonomic data and lipid profiles

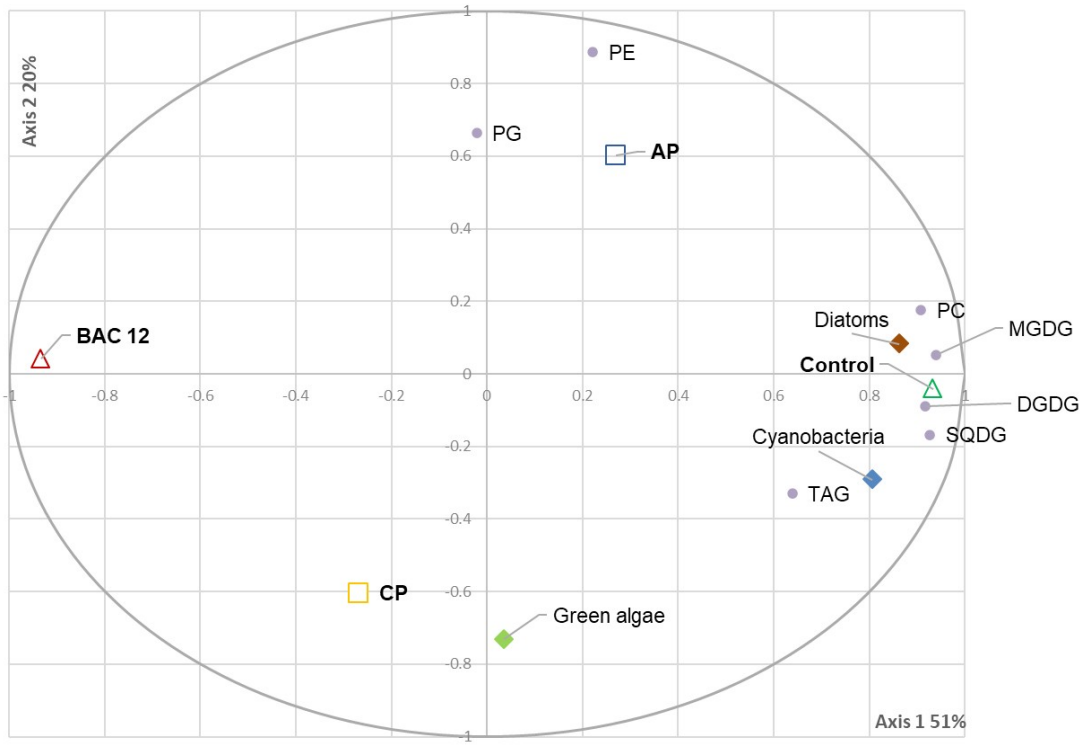

Figure 3: Principal component analysis conducted on lipid and taxonomic data at d0, d1, d2 and d10. BAC 12 = contaminated biofilm; AP = alternated photoperiod CP = continuous photoperiod; PE = phosphatidylethanolamine; PC = phosphatidylcholine; PG = phosphatidylglycerol; DGDG = digalactosyldiacylglycerol; MGDG = monogalactosyldiacylglycerol; SQDG = sulfoquinovosyldiacylglycerol; TAG = triacylglycerides.

The principal component analysis (Figure 3) illustrates the relationships between the different lipid classes, the three taxonomic groups present in the biofilms and the two stressors (light and BAC 12). Axis 1 explains 51% of the total variance and shows an anticorrelation between the presence of the three classes of glycolipids (i.e. SQDG, DGDG and MGDG) and BAC 12 exposure. Diatom and cyanobacteria densities are also negatively correlated with BAC 12 exposure and positively correlated with glycolipids. Both TAG and PC cluster with diatoms. The second axis explains 20% of the total variance and shows how higher densities of green algae are associated with continuous light. PE and PG, associated with axis 2, are not specific and can also be found in bacteria, which were not considered in this study.

15

3.5- BAC 12 bioaccumulation in biofilms

Table 4. Evolution of BAC 12 bioaccumulated in biofilms (expressed in log(BCF)) between the different photoperiod treatments for the hydrophilic fraction of lipidomic samples only. AP = alternated photoperiod CP = continuous photoperiod

	d1	d2	d10
AP	2.18 ± 1.70	3.03 ± 0.34	3.40 ± 0.10
CP	3.23 ± 0.30	2.90 ± 0.98	3.33 ± 0.10

Table 4 shows the log(BCF) for the hydrophilic fraction at d1, d2 and d10 for the two photoperiod conditions. BAC 12 was recovered from biofilms for every treatment and every sampling time, showing that this compound bioaccumulates well in algal biofilms, with a mean log(BCF) of 3.22 ± 0.25. The amount of BAC 12 bioaccumulated in the biofilms showed no significant difference between sampling dates ($F_{[2,28]}$= 2.38; p= 0.11) and no significant difference in bioaccumulation was found between the two photoperiod treatments ($F_{[1,28]}$ = 0.28; p = 0.60). Overall, the amount of BAC 12 bioaccumulated in biofilms was stable through the experiment with no significant difference was found between the two photoperiod treatments ($F_{[2,28]}$ = 0.025; p = 0.98)

4. Discussion

4.1- Experimental conditions and contamination

BAC 12 seemed to have an indirect effect on nutrient concentrations over the 10-day exposure period of our experiment, possibly by affecting biofilm microorganisms (reduced growth). BAC 12 concentrations in the channels under the continuous photoperiod significantly decreased over time. This could be the result of photodegradation of the contaminant. A previous study showed that freshwater biofilms can improve the photodegradation of organic contaminants by being a source of reactive oxygen species (ROS) such as hydroxyl (OH·) or superoxide (O2·) radicals (Yin et al. 2022). Contrary to the hypothesis of Pozo-Antonio and Sanmartin (2018), who suggested that artificial light could lead to an increase in internalization of the contaminant, we found no significant difference in BAC12 concentrations in biofilm between the different light conditions (Table 2). Thus, our results do not support the hypothesis of a higher uptake of the substance from the water through increased bioaccumulation under continuous light exposure. This lower concentration might be linked to some bacterial strains such as *Aeromonas hydrophila* that can biodegrade BAC 12 and use the degradation product as an energy source (Patrauchan

16

436 and Oriel, 2003). However, resistant strains cannot withstand BAC 12 concentrations higher
437 than 10 mg.L^{-1} (Kreuzinger et al., 2007).

438 **4.2- Effects of BAC 12 on the biofilm**

439 The first effect of BAC 12 observed was the marked and rapid decrease in photosynthetic
440 efficiency (more than 90% compared with the initial yield; Figure 1). This sudden inhibition of
441 photosynthesis was not expected because the exposure concentration was based on the EC_5
442 for photosynthesis inhibition after 4 hours of exposure determined in a preliminary
443 experiment (EC_5 = 30 mg.L^{-1}; Figure A).

444 Based on our microscopic observations, diatom mortality was low in our samples (<10%) and
445 not significantly different from the controls. It should be noted that only diatoms that no
446 longer had chlorophyll in their cell content (Morin et al. 2010) were considered as dead cells
447 in our study, while cells with chloroplasts were counted as live diatoms. However, many of
448 the cells where content was observed nevertheless seemed to have suffered critical
449 alteration of their photosynthetic equipment (Figure B.2). Their integrity was potentially
450 severely affected, which could explain the loss of photosynthetic yield in biofilms exposed to
451 BAC 12. This deterioration of cell integrity may be due to the fact that BAC 12 is able to
452 quickly penetrate the cell (Severina et al. 2001).

453 The striking decrease in lipid content in biofilms exposed to BAC 12, particularly glycolipids
454 found mainly in thylakoid membranes within photosynthetic cells (Zulu et al., 2018),
455 supports the idea that the contaminant is internalized within cells. The degradation of the
456 photosynthetic material observed microscopically (Figure B.2) in turn explains the alteration
457 of photosynthesis. In parallel to this decrease in glycolipids with BAC 12 contamination, we
458 observed an increase in phospholipids. It is difficult to clearly explain this increase because
459 the phospholipid groups analysed (i.e. PE, PC and PG) are not specific to any taxonomic
460 group and can be found in both the plasma membranes of microalgae (Zulu et al., 2018) and
461 in prokaryotic cells (Li-Beisson et al., 2013). One hypothesis to explain this increase could be
462 the development of BAC 12-resistant bacteria. Indeed, the mechanism of resistance to
463 benzalkonium chloride identified in *Pseudomonas aeruginosa* consists of an increase in the
464 percentage of phospholipids (Sakagami et al. 1989).

465 Sensitivity to BAC 12 differed among algal taxa, whose proportions changed over time, and
466 with BAC 12 concentration. This result suggests that the biofilm community acclimated to
467 the chemical stress and that only resistant/tolerant species survived BAC 12 exposure.
468 Diatoms appeared to be minimally affected based on growth and mortality, even though
469 their photosynthetic structure and cell content was altered (Figure B.2). Green algae, which
470 experienced rapid growth in non-contaminated channels, appeared to be negatively affected
471 by BAC 12 at d10. BAC 12 also had a strong effect on heterotrophic microfauna naturally
472 present in the biofilms (e.g. rotifers, tardigrades), suggesting that they are highly sensitive to
473 this contaminant.

474

475

476

477

478 **4.3- Effects of ALAN on the biofilm**

479 The continuous photoperiod did not significantly modify the structure or physiology of the
480 autotrophic organisms in the biofilm based on the parameters that we investigated.
481 Although the continuous photoperiod did not result in growth differences among diatoms,
482 green algae and cyanobacteria, the ordination (Figure 3) suggests that ALAN could benefit
483 green algae, as already demonstrated in some previous studies (Yang et al., 2012; Ugwu et
484 al., 2007).

485

486 It would also be of interest to perform more in-depth lipid analysis to determine whether
487 fatty acids show a clearer difference between light conditions than was visible from a global
488 assessment of lipid classes. Amini Khoeyi et al. (2011), studying *Chlorella vulgaris*, showed
489 that a prolonged photoperiod can decrease microalgal content of monounsaturated (MUFA)
490 and polyunsaturated (PUFA) fatty acids. Such a decrease could be enhanced by BAC 12
491 activity, which can disrupt lipid membranes and degrade lipids, thereby
492 possibly exacerbating the negative effect of the prolonged photoperiod on MUFA and PUFA
493 content. A decrease in essential polyunsaturated fatty acids, such as certain omega-3 and
494 omega-6 types, could alter the nutritional quality of biofilms and decrease the energy supply
495 along the trophic chain (Brett and Müller-Navarra; 1997). Concerning the polar lipid classes,
496 an increase of MGDG or DGDG is often observed during low light intensity exposures
497 (Gushina and Harwood, 2009). In the present experiment, while the light intensity remained
498 the same, the duration of exposure varied, which could explain the absence of a significant
499 effect on these two glycolipids over time. Conversely, high light levels can lead to a decrease
500 in polar lipids, especially phospholipids, in favour of TAGs, especially in the case of
501 filamentous green algae such as *Cladophora* spp. Such a phenomenon was not clearly
502 observed here, which could be due to compensation phenomena or to our averaging of the
503 lipid mixture across different organisms present within a natural biofilm, which differs from
504 the analysis of an isolated chlorophyte strain.

505

506

507 **4.4- Combined effects of BAC and ALAN on the biofilm**

508 Contrary to our hypotheses, BAC 12 and ALAN exposure did not show interaction effects on
509 any of the parameters monitored in this experiment. However, continuous light impacted
510 the fate of BAC 12 by decreasing exposure concentrations in the medium. As the high
511 concentration of BAC 12 tested drove most of the changes observed in biofilm composition
512 and physiology, we cannot exclude that BAC 12 exposure masked possible interactions
513 between the stressors. Further experiments combining lower concentrations of BAC 12 with
514 ALAN would be required to completely rule out any interaction effects on aquatic biofilms.

515

516

517

5- Conclusion

In this experiment, we demonstrated that BAC 12 exposure strongly impacts biofilms. The damage to the quality and quantity of photosynthetic pigments following BAC 12 exposure implies a serious impact on the photosynthetic efficiency of the biofilm. There was also evidence for an impact on the structure of the biofilm as changes in its taxonomic composition were observed. Indeed, even though the mortality index did not show greater mortality in the exposed diatoms compared with the controls, microscopic observations suggest that a marked number of individuals were strongly impacted on a physiological level (degraded cell content) and were potentially not viable. This hypothesis is supported by the results obtained during the lipidomic analysis, highlighting a strong decrease in the lipid classes associated with thylakoid membranes specific to microalgae.

In contrast, ALAN did not lead to any significant change in biofilms, even though the ALAN conditions modified their exposure to BAC 12. In view of the increased use of BAC 12 in the context of the Covid-19 pandemic and the likely increase in its concentration in urban waters (downstream of WWTPs) where ALAN is often common, it would also be necessary to investigate whether the effects identified in the present study are manifested at environmental concentrations in order to reassess the risk posed by BAC 12 to aquatic biodiversity.

Aknowledgements

The authors aknowledge the financial support from the Institut National de Recherche pour l'Agriculture, l'alimentation et l'Environnement (INRAE), l'Institut National de la Recherche Scientifique (INRS) and the Groupe de Recherche Interuniversitaire en Limnologie (GRIL).

19

References

Abbott, T., Kor-Bicakci, G., Islam, M.S., Eskicioglu, C., 2020. A Review on the Fate of Legacy and Alternative Antimicrobials and Their Metabolites during Wastewater and Sludge Treatment. International Journal of Molecular Sciences 21, 9241. https://doi.org/10.3390/ijms21239241

Amini Khoeyi, Z., Seyfabadi, J., Ramezanpour, Z., 2012. Effect of light intensity and photoperiod on biomass and fatty acid composition of the microalgae, Chlorella vulgaris. Aquacult Int 20, 41–49. https://doi.org/10.1007/s10499-011-9440-1

Brett, M., Müller-Navarra, D., 1997. The role of highly unsaturated fatty acids in aquatic foodweb processes. Freshwater Biology 38, 483–499. https://doi.org/10.1046/j.1365-2427.1997.00220.x

Chaumet, B., Morin, S., Hourtané, O., Artigas, J., Delest, B., Eon, M., Mazzella, N., 2019. Flow conditions influence diuron toxicokinetics and toxicodynamics in freshwater biofilms. Science of The Total Environment 652, 1242–1251. https://doi.org/10.1016/j.scitotenv.2018.10.265

Chen, Y., Geurts, M., Sjollema, S.B., Kramer, N.I., Hermens, J.L.M., Droge, S.T.J., 2014. Acute toxicity of the cationic surfactant C12-benzalkonium in different bioassays: How test design affects bioavailability and effect concentrations. Environmental Toxicology and Chemistry 33, 606–615. https://doi.org/10.1002/etc.2465

Clara, M., Scharf, S., Scheffknecht, C., Gans, O., 2007. Occurrence of selected surfactants in untreated and treated sewage. Water Research 41, 4339–4348. https://doi.org/10.1016/j.watres.2007.06.027

Demailly, F., Elfeky, I., Malbezin, L., Le Guédard, M., Eon, M., Bessoule, J.-J., Feurtet-Mazel, A., Delmas, F., Mazzella, N., Gonzalez, P., Morin, S., 2019. Impact of diuron and S-metolachlor on the freshwater diatom Gomphonema gracile: Complementarity between fatty acid profiles and different kinds of ecotoxicological impact-endpoints. Science of The Total Environment 688, 960–969. https://doi.org/10.1016/j.scitotenv.2019.06.347

Ech, J., Dürholt, H., Steger-Hartmann, T., Wagner, E., 2000. Specific Detection of Membrane-Toxic Substances with a Conductivity Assay. Ecotoxicology and Environmental Safety 45, 228–235. https://doi.org/10.1006/eesa.1999.1854

Falchi, F., Cinzano, P., Duriscoe, D., Kyba, C.C.M., Elvidge, C.D., Baugh, K., Portnov, B.A., Rybnikova, N.A., Furgoni, R., n.d. The new world atlas of artificial night sky brightness. Science Advances 2, e1600377. https://doi.org/10.1126/sciadv.1600377

Grubisic, M., Singer, G., Bruno, M.C., Grunsven, R.H.A. van, Manfrin, A., Monaghan, M.T., Hölker, F., 2017. Artificial light at night decreases biomass and alters community composition of benthic primary producers in a sub-alpine stream. Limnology and Oceanography 62, 2799–2810. https://doi.org/10.1002/lno.10607

Kreuzinger, N., Fuerhacker, M., Grillitsch, B., Scharf, S., Uhl, M., Gans, O., 2007. Methodological approach towards the environmental significance of uncharacterized substances — quaternary ammonium compounds as an example. Desalination 215, 209–222. https://doi.org/10.1016/j.desal.2006.10.036

20

Patrauchan, M.A., Oriel, P.J., 2003. Degradation of benzyldimethylalkylammonium chloride by Aeromonas hydrophila sp. K. J. Appl. Microbiol. 94, 266–272. https://doi.org/10.1046/j.1365-2672.2003.01829.x

Kahrilas, G.A., Blotevogel, J., Stewart, P.S., Borch, T., 2015. Biocides in Hydraulic Fracturing Fluids: A Critical Review of Their Usage, Mobility, Degradation, and Toxicity. Environ. Sci. Technol. 49, 16–32. https://doi.org/10.1021/es503724k

Kim, M., Hatt, J.K., Weigand, M.R., Krishnan, R., Pavlostathis, S.G., Konstantinidis, K.T., 2018. Genomic and Transcriptomic Insights into How Bacteria Withstand High Concentrations of Benzalkonium Chloride Biocides. Appl. Environ. Microbiol. 84. https://doi.org/10.1128/AEM.00197-18

Kreuzinger, N., Fuerhacker, M., Scharf, S., Uhl, M., Gans, O., Grillitsch, B., 2007. Methodological approach towards the environmental significance of uncharacterized substances — quaternary ammonium compounds as an example. Desalination 215, 209–222. https://doi.org/10.1016/j.desal.2006.10.036

Kümmerer, K., Eitel, A., Braun, U., Hubner, P., Daschner, F., Mascart, G., Milandri, M., Reinthaler, F., Verhoef, J., 1997. Analysis of benzalkonium chloride in the effluent from European hospitals by solid-phase extraction and high-performance liquid chromatography with post-column ion-pairing and fluorescence detection. Journal of Chromatography A 774, 281–286. https://doi.org/10.1016/S0021-9673(97)00242-2

Lavorgna, M., Russo, C., D'Abrosca, B., Parrella, A., Isidori, M., 2016. Toxicity and genotoxicity of the quaternary ammonium compound benzalkonium chloride (BAC) using Daphnia magna and Ceriodaphnia dubia as model systems. Environmental Pollution 210, 34–39. https://doi.org/10.1016/j.envpol.2015.11.042

Leal, J.S., González, J.J., Kaiser, K.L.E., Palabrica, V.S., Comelles, F., García, M.T., 1994. On the Toxicity and Biodegradation of Cationic Surfactants Über die Toxizität und den biologischen Abbau kationischer Tenside. Acta hydrochimica et hydrobiologica 22, 13–18. https://doi.org/10.1002/aheh.19940220105

Li-Beisson, Y., Shorrosh, B., Beisson, F., Andersson, M.X., Arondel, V., Bates, P.D., Baud, S., Bird, D., DeBono, A., Durrett, T.P., Franke, R.B., Graham, I.A., Katayama, K., Kelly, A.A., Larson, T., Markham, J.E., Miquel, M., Molina, I., Nishida, I., Rowland, O., Samuels, L., Schmid, K.M., Wada, H., Welti, R., Xu, C., Zallot, R., Ohlrogge, J., 2013. Acyl-Lipid Metabolism. arbo.j 2013. https://doi.org/10.1199/tab.0161

Longcore, T., Rich, C., 2004. Ecological light pollution. Frontiers in Ecology and the Environment 2, 191–198. https://doi.org/10.1890/1540-9295(2004)002[0191:ELP]2.0.CO;2

Lorenzen, C.J., 1967. Determination of chlorophyll and pheo-pigments: Spectrophotometric equations. Limnol. Oceanogr. 12, 343–346. https://doi.org/10.4319/lo.1967.12.2.0343

Maggi, E., Serôdio, J., 2020. Artificial Light at Night: A New Challenge in Microphytobenthos Research. Front. Mar. Sci. 7. https://doi.org/10.3389/fmars.2020.00329

Martínez-Carballo, E., Sitka, A., González-Barreiro, C., Kreuzinger, N., Fürhacker, M., Scharf, S., Gans, O., 2007. Determination of selected quaternary ammonium compounds by liquid chromatography with mass spectrometry. Part I. Application to surface, waste and indirect discharge water samples in Austria. Environmental Pollution 145, 489–496. https://doi.org/10.1016/j.envpol.2006.04.033

Morin, S., Proia, L., Ricart, M., Bonnineau, C., Geiszinger, A., Ricciardi, F., Guasch, H., Romani, A.M., Sabater, S., 2010. Effects of a bactericide on the structure and survival of benthic diatom communities. Vie et Milieu / Life & Environment 60, 109.

21

Neury-Ormanni, J., Vedrenne, J., Wagner, M., Jan, G., Morin, S., 2020. Micro-meiofauna morphofunctional traits linked to trophic activity. Hydrobiologia 847, 2725–2736. https://doi.org/10.1007/s10750-019-04120-0

Patrauchan, M.A., Oriel, P.J., 2003. Degradation of benzyldimethylalkylammonium chloride by Aeromonas hydrophila sp. K. Journal of Applied Microbiology 94, 266–272. https://doi.org/10.1046/j.1365-2672.2003.01829.x

Pérez, P., Fernández, E., Beiras, R., 2009. Toxicity of Benzalkonium Chloride on Monoalgal Cultures and Natural Assemblages of Marine Phytoplankton. Water Air Soil Pollut 201, 319–330. https://doi.org/10.1007/s11270-008-9947-x

Perkin, E.K., Hölker, F., Richardson, J.S., Sadler, J.P., Wolter, C., Tockner, K., 2011. The influence of artificial light on stream and riparian ecosystems: questions, challenges, and perspectives. Ecosphere 2, art122. https://doi.org/10.1890/ES11-00241.1

Pozo-Antonio, J.S., Sanmartín, P., 2018. Exposure to artificial daylight or UV irradiation (A, B or C) prior to chemical cleaning: an effective combination for removing phototrophs from granite. Biofouling 34, 851–869. https://doi.org/10.1080/08927014.2018.1512103

R Core Team (2020). — European Environment Agency [WWW Document], n.d. URL https://www.eea.europa.eu/data-and-maps/indicators/oxygen-consuming-substances-in-rivers/r-development-core-team-2006 (accessed 10.31.22).

Rabenau, H.F., Kampf, G., Cinatl, J., Doerr, H.W., 2005. Efficacy of various disinfectants against SARS coronavirus. Journal of Hospital Infection 61, 107–111. https://doi.org/10.1016/j.jhin.2004.12.023

Sakagami, Y., Yokoyama, H., Nishimura, H., Ose, Y., Tashima, T., 1989. Mechanism of resistance to benzalkonium chloride by Pseudomonas aeruginosa. Appl Environ Microbiol 55, 2036–2040.

Severina, I.I., Muntyan, M.S., Lewis, K., Skulachev, V.P., 2001. Transfer of Cationic Antibacterial Agents Berberine, Palmatine, and Benzalkonium Through Bimolecular Planar Phospholipid Film and Staphylococcus aureus Membrane. IUBMB Life 52, 321–324. https://doi.org/10.1080/152165401317291183

Singh, S.P., Singh, P., 2015. Effect of temperature and light on the growth of algae species: A review. Renew. Sustain. Energy Rev. 50, 431–444. https://doi.org/10.1016/j.rser.2015.05.024

Sreevidya, V.S., Lenz, K.A., Svoboda, K.R., Ma, H., 2018. Benzalkonium chloride, benzethonium chloride, and chloroxylenol - Three replacement antimicrobials are more toxic than triclosan and triclocarban in two model organisms. Environmental Pollution 235, 814–824. https://doi.org/10.1016/j.envpol.2017.12.108

Stutterlin, H., Alexy, R., Kümmerer, K., 2008. The toxicity of the quaternary ammonium compound benzalkonium chloride alone and in mixtures with other anionic compounds to bacteria in test systems with Vibrio fischeri and Pseudomonas putida. Ecotoxicology and Environmental Safety 71, 498–505. https://doi.org/10.1016/j.ecoenv.2007.12.015

Tamminen, M., Spaak, J., Tlili, A., Eggen, R., Stamm, C., Räsänen, K., 2022. Wastewater constituents impact biofilm microbial community in receiving streams. Science of The Total Environment 807, 151080. https://doi.org/10.1016/j.scitotenv.2021.151080

Tlili, A., Corcoll, N., Arrhenius, Å., Backhaus, T., Hollender, J., Creusot, N., Wagner, B., Behra, R., 2020. Tolerance Patterns in Stream Biofilms Link Complex Chemical Pollution to Ecological Impacts. Environ. Sci. Technol. 54, 10745–10753. https://doi.org/10.1021/acs.est.0c02975

Ugwu, C.U., Aoyagi, H., Uchiyama, H., 2007. Influence of irradiance, dissolved oxygen concentration, and temperature on the growth of Chlorella sorokiniana. Photosynthetica 45, 309–311. https://doi.org/10.1007/s11099-007-0052-y

22

10 United States Environmental Protection Agency 2006. Reregistration eligibility decision for alkyl dimethyl benzyl ammonium chloride. (https://nepis.epa.gov). Accessed on 17 Feb. 2021.

11 US EPA, O., 2020. About List N: Disinfectants for Coronavirus (COVID-19) [WWW Document]. URL https://www.epa.gov/coronavirus/about-list-n-disinfectants-coronavirus-covid-19-0 (accessed 10.31.22).

12 Van Wijk, D., Gyimesi-van den Bos, M., Garttener-Arends, I., Geurts, M., Kamstra, J., Thomas, P., 2009. Bioavailability and detoxification of cationics: I. Algal toxicity of alkyltrimethyl ammonium salts in the presence of suspended sediment and humic acid. Chemosphere 75, 303–309. https://doi.org/10.1016/j.chemosphere.2008.12.047

13 Wassenaar, T., Ussery, D., Nielsen, L., Ingmer, H., 2015. Review and phylogenetic analysis of qac genes that reduce susceptibility to quaternary ammonium compounds in Staphylococcus species. European Journal of Microbiology and Immunology 5, 44–61. https://doi.org/10.1556/eujmi-d-14-00038

14 Yang, Z., Geng, L., Wang, W., Zhang, J., 2012. Combined effects of temperature, light intensity, and nitrogen concentration on the growth and polysaccharide content of Microcystis aeruginosa in batch culture. Biochem. Syst. Ecol. 41, 130–135. https://doi.org/10.1016/j.bse.2011.12.015

15 Yin, H., Wang, Lingling, Zeng, G., Wang, Longfei, Li, Y., 2022. The Roles of Different Fractions in Freshwater Biofilms in the Photodegradation of Methyl Orange and Bisphenol A in Aqueous Solutions. Int. J. Environ. Res. Public. Health 19, 12995. https://doi.org/10.3390/ijerph192012995

16 Zhang, C., Cui, F., Zeng, G., Jiang, M., Yang, Z., Yu, Z., Zhu, M., Shen, L., 2015. Quaternary ammonium compounds (QACs): A review on occurrence, fate and toxicity in the environment. Science of The Total Environment 518–519, 352–362. https://doi.org/10.1016/j.scitotenv.2015.03.007

17 Zulu, N.N., Zienkiewicz, K., Vollheyde, K., Feussner, I., 2018. Current trends to comprehend lipid metabolism in diatoms. Progress in Lipid Research 70, 1–16. https://doi.org/10.1016/j.plipres.2018.03.001

23

Appendices

A- Preliminary experiment

This preliminary experiment aimed to test the sensitivity of our biofilm to dodecylbenzyldimethylammonium (BAC 12) to select a sub-lethal concentration to be used in the main experiment. We ran a dose-response experiment in which we tested nine concentrations ranging between 17.5 µg.L^{-1} and 175 mg.L^{-1} (following a logarithmic increase) for 4 hours. Each concentration was tested twice, one test at a mean light level of 16.86 µmol.s.m^{-2} and the other kept in the dark.

Glass slides (26.5 cm × 6 cm) colonized by biofilms for three months were scraped and the biofilms put into 500 mL of water. For each concentration, we contaminated 1.5 mL of the biofilm solution. After four hours of contamination, we analysed the photosynthetic efficiency of the samples with a Phyto-PAM (see section 2.3).

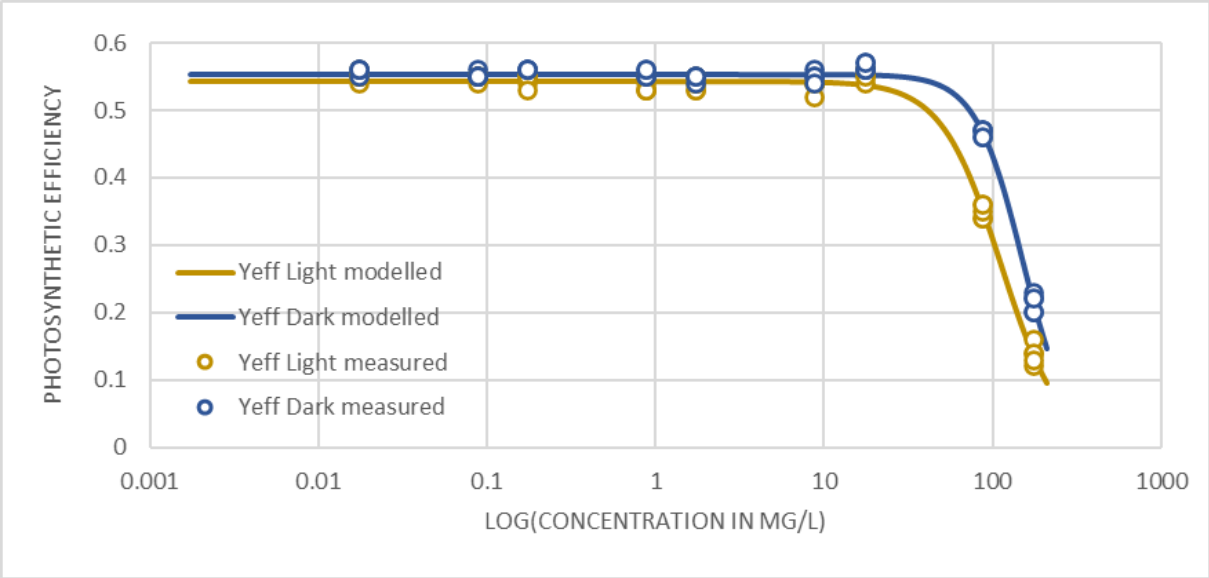

Figure A. Dose-Response curve for photosynthetic efficiency in biofilms exposed to light or dark and increasing BAC concentration for 4 hours. Yeff = Photosynthetic efficiency.

The dose-response curve give us an EC_{50} of 112 ± 3 mg.L^{-1} and a EC_5 of 34 ± 3 mg.L^{-1} for photosynthesis inhibition in biofilm exposed to light. For the biofilm kept in obscurity, we found EC_{50} of 151 ± 3 mg.L^{-1} and a EC_5 of 58 ± 3 mg.L^{-1}. This result allowed us to choose the

24

concentration of 30 mg.L^{-1} for the 10 days biofilm exposure which is the lowest concentration with a minimum effect on photosynthetic efficiency.

B- Effects of BAC 12 on chloroplasts

Figure B.1. Chloroplasts of diatoms in non-contaminated biofilm. x400 magnification

25

Figure B.2. Chloroplasts of diatoms in BAC 12 contaminated biofilm after 10 days of exposure. x400 magnification.

C- Pigment analysis

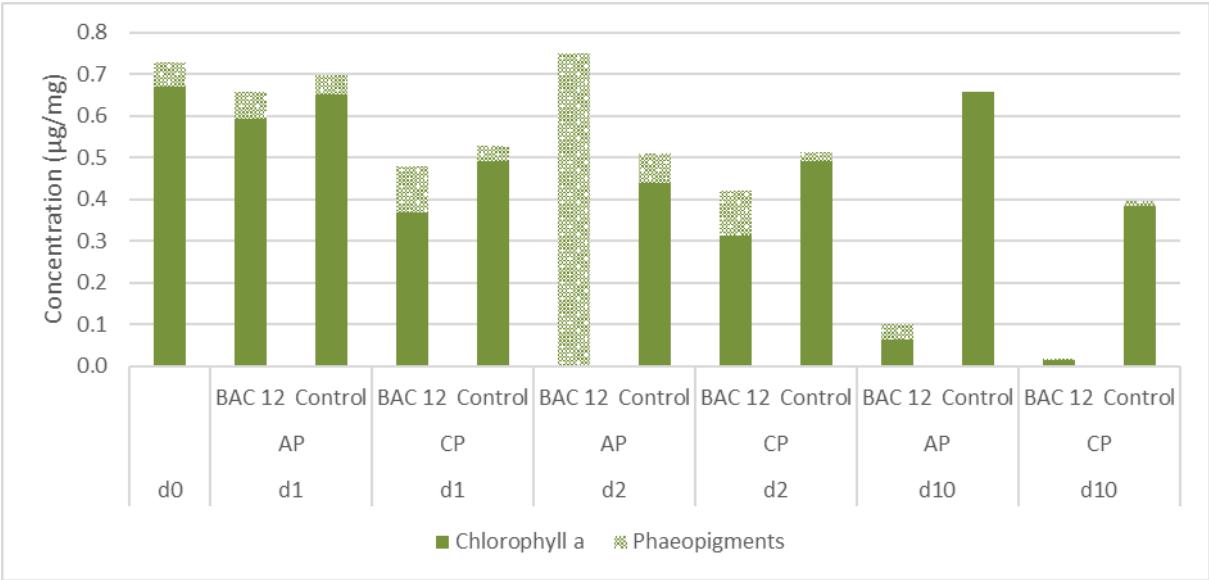

Figure C. Pigment analysis. n = 1. BAC 12 = contaminated biofilm; Control = non-exposed biofilm; AP = alternated photoperiod; CP = continuous photoperiod.

Although the pigment analyses were only performed on one replicate, we can see that chlorophyll *a* concentrations are lower in the BAC 12 contaminated samples than in the

26

control samples. At d2, we see that there is no chlorophyll a in the contaminated samples for AP but only phaeopigments. At the end of the experiment, there were very low pigment concentrations in contaminated samples. Due to the lack of replicates, we cannot assess whether there were significant effects of light conditions, BAC 12 contamination or any interaction between light, BAC 12 and/or time on chlorophyll *a* or phaeopigment levels.

D- HPLC gradients for the lipidomic analysis

Table D.1. HPLC gradients for phospholipid and glycolipid analysis.

Time (min)	40 mmol.L^{-1} Ammonium acetate buffer (%)	Acetonitrile (%)
0	5	95
2	5	95
7	30	70
10	30	70
11	5	95

27

13.7	5	95

816

817 **Table D.2. HPLC gradients for triglyceride analysis.**

818

Time (min)	Solvent A* (%)	Solvent B* (%)
0	50	50
0.3	50	50
5.3	1	99
7.3	1	99
8.3	50	50
9.8	50	50

819 * Solvent A: solution of acetonitrile/water/40 mmol.L^{-1} ammonium acetate buffer
820 (600/390/10, v/v/v)

821 Solvent B: solution of isopropanol/acetonitrile/1 mol.L^{-1} ammonium acetate buffer
822 (900/90/10, v/v/v)

823

824 **E- Lipid standards**

825 Polar lipid standards were purchased from Avanti Polar Lipids. Quantitations of
826 phosphatidylcholine (PC), phosphatidylethanolamine (PE) and phosphatidylglycerol (PG)
827 were respectively carried out with 1-palmitoyl-2-oleoyl-glycero-3-phosphocholine or PC
828 (16:0/18:1) (850457), 1-palmitoyl-2-oleoyl-sn-glycero-3-phosphoethanolamine or PE
829 (16:0/18:1) (850757), and 1-palmitoyl-2-oleoyl-sn-glycero-3-phospho-(1'-rac-glycerol) or PG
830 (16:0/18:1) (840457).

831 For glycolipids, monogalactosyldiacylglycerol (840523), digalactosyldiacylglycerol (840524)
832 and sulfoquinovosyldiacylglycerol (840525) from plant extracts were used as standards.
833 Quantitation was performed with the following molecular species: MGDG (16:3_18:3) (63%

of the total MGDG standard), DGDG (18:3_18:3) (22% of the total MGDG standard), and SQDG (34:3) (78% of the total MGDG standard).

1,2-diheptadecanoyl-sn-glycero-3-phosphocholine or PC (2x17:0) (850360) was used as internal standard for PC phospholipids, 1,2-diheptadecanoyl-sn-glycero-3-phosphoethanolamine or PE (2x17:0) (830756) was used as internal standard for PE phospholipids, and 1,2-diheptadecanoyl-sn-glycero-3-phospho-(1'-rac-glycerol) or PG (2x17:0) (830456) was used as internal standard for PG phospholipids, and both MGDG, DGDG and SQDG glycolipids.

1,2-dipalmitoyl-sn-glycero-3-O-4'-(N,N,N-trimethyl)-homoserine or DGTS (2x16:0) (857464) was used for the diacylglyceryltrimethylhomo-Ser (DGTS) lipids. 1,2-dipalmitoyl-sn-glycero-3-O-4'-[N,N,N-trimethyl(d9)]-homoserine or DGTS-d9 (2x16:0) (857463) was used as internal standard for DGTS lipids

Triglycerides were purchased from Sigma-Aldrich. Tristearin or TAG (3x18:0) (≥99%, T5016) was used as the calibration standard while TAG (3x17:0) (≥99%, T2151) was used as the internal standard.

F- Mass spectrometry parameters for lipid analysis

Table F.1. Mass spectrometry parameters for phospholipid and glycolipid analysis.

	Curtain gas	CAD	IonSpray	Temperature	Ion source gas 1	Ion source gas 2	Declustering potential	Collision energy
MGDG	30 psi	3	-4500 V	450°C	30 psi	60 psi	-61 V	-28 V
DGDG	30 psi	3	-4500 V	450°C	30 psi	60 psi	-61 V	-28 V
SQDG	30 psi	3	-4500 V	450°C	30 psi	60 psi	-126 V	-66 V
PE	30 psi	3	-4500 V	450°C	30 psi	60 psi	-50 V	-50 V

29

PG	30 psi	3	-4500 V	450°C	30 psi	60 psi	-100 V	-50 V
PC	30 psi	3	-4500 V	450°C	30 psi	60 psi	-100 V	-50 V

Table F.2. Mass spectrometry parameters for triglyceride analysis.

	Curtain gas	CAD	IonSpray	Temperature	Ion source gas 1	Ion source gas 2	Declustering potential	Collision energy
Triglycerides	30 psi	3	+5000 V	450°C	30 psi	45 psi	50 V	38 V

30